Fructus *Ligustri Lucidi* inhibits ferroptosis in ovariectomy-induced osteoporosis in rats via the Nrf2/HO-1 signaling pathway

PEI LI*, YUHAN WANG*, QIQI YAN, YING YANG, RUYUAN ZHU, JIAYI MA, YANJING CHEN, HAIXIA LIU and ZHIGUO ZHANG

Institute of Basic Theory for Chinese Medicine, China Academy of Chinese Medical Sciences, Beijing 100700, P.R. China

Received September 18, 2023; Accepted November 20, 2023

DOI: 10.3892/br.2023.1715

Abstract. Postmenopausal osteoporosis (PMOP) has increased in prevalence in recent years, thus researchers have evaluated alternative medicine therapies. Fructus *Ligustri Lucidi* (FLL) can inhibit bone loss, and ferroptosis serves an important role in osteoporosis. Therefore, the present study assessed the presence of ferroptosis in PMOP and whether FLL could inhibit ferroptosis to improve bone microstructure in ovariectomized rats. Ovariectomized rats were treated with FLL (1.56 g/kg/day) for 12 weeks. Micro-CT was performed to evaluate the bone microstructure and bone mineral density. Western blotting and reverse transcription-quantitative PCR were performed to assess the relative expression levels of proteins and mRNA. Subsequently, malondialdehyde (MDA) and Fe^{2+} assay kits were used to quantify the MDA and Fe^{2+} content, respectively. The results demonstrated that ovariectomy (OVX) resulted in iron overload and the accumulation of lipid peroxide. Furthermore, the expression of key factors that inhibited ferroptosis, glutathione peroxidase 4 and solute carrier family 7 member 11 was significantly downregulated in ovariectomized rats, which was significantly reversed by FLL treatment. Furthermore, bone formation was assessed using the expression of osteogenesis-related genes, runt-related transcription factor 2 and osterix, which revealed significantly higher levels in FLL-treated rats compared with ovariectomized rats. The levels of nuclear factor erythroid 2-related factor 2 (Nrf2) and heme oxygenase-1 (HO-1) were also significantly recovered following FLL treatment. In the present study, OVX of postmenopausal osteoporotic rats was found to induce ferroptosis by enhancing lipid peroxidation and Fe^{2+} levels. FLL significantly suppressed ferroptosis, protected the osteogenic ability of ovariectomized rats and promoted the Nrf2/HO-1 signaling pathway.

Correspondence to: Professor Zhiguo Zhang or Miss Haixia Liu, Institute of Basic Theory for Chinese Medicine, China Academy of Chinese Medical Sciences, 16 Nanxiao Street, Dongzhimennei, Dongcheng District, Beijing 100700, P.R. China
E-mail: zzgtcm@163.com
E-mail: lhx8866_7@163.com

*Contributed equally

Key words: Fructus *Ligustri Lucidi*, osteoporosis, ovariectomy, ferroptosis, nuclear factor erythroid 2-related factor 2/heme oxygenase-1 pathway

Introduction

Osteoporosis (OP) is one of the most common metabolic bone diseases and is characterized by loss of trabecular bone, destruction of the bone microarchitecture and decreased bone strength, and presents an increasing prevalence in postmenopausal women (1). In a survey in 2017-2018 in China, the prevalence of OP in postmenopausal women was 32.1% (2). According to another survey in the 27 countries of the European Union (EU27), 22 million women were estimated to have OP (3). Postmenopausal OP (PMOP) is mainly attributed to a lack of estrogen and is associated with iron overload and oxidative stress. These conditions affect bone homeostasis and lead to chronic loss of trabecular bone, increased bone fragility and a high risk of fracture (4). As the most severe clinical outcome of OP, osteoporotic fractures are associated with high morbidity and mortality, and are emerging as a major global public health problem (5). The probability of women at the age of 50 years developing osteoporotic fractures during their remaining lifespan is 46%. It was estimated that in the EU27 in 2010 the number of deaths directly attributable to fracture was at 24 per 100,000 people at risk (aged ≥50 years) (3). Current treatment options such as selective estrogen receptor modulators and other therapeutic approaches for OP, have limitations, including causing other illness and adverse reactions (6). With increased demand for alternative medicine, medicinal plants have been reported as potential therapeutic options for the prevention and treatment of OP (7).

Ferroptosis is a form of programmed cell death that is characterized by iron-dependent accumulation of lipid peroxidation, and impaired cell membrane structure and function (8). In terms of morphology, cells are round, small and scattered; mitochondria are small, with increased mitochondrial membrane density, reduction or loss of mitochondrial cristae and ruptured mitochondrial outer membrane (9). Furthermore, the cystine-glutamate antiporter (System Xc-)/glutathione

peroxidase 4 (GPX4) axis serves an essential role in inhibiting ferroptosis (10). Previous studies have suggested that ferroptosis is related to the regulation of bone metabolism via regulation of the metabolism of osteocytes (11,12). It has also been reported that iron overload is positively associated with the pathogenesis of OP (13). Postmenopausal women often suffer from iron overload, and decreasing iron intake or administering iron chelator treatment can improve bone microstructure and prevent bone loss (4). Furthermore, it has been reported that in women aged ≥45 years, serum ferritin concentrations are inversely associated with lumbar bone mineral density (BMD), femur neck BMD and total femur BMD (14). Furthermore, iron overload promotes the formation of reactive oxygen species (ROS), which exert further stress on bones (11). Therefore, ferroptosis could markedly influence the pathogenesis of PMOP.

Fructus *Ligustri Lucidi* (FLL) has been used in Traditional Chinese Medicine for the treatment of bone diseases and is still used in the treatment of OP (15). Pharmacological studies have reported that FLL can promote differentiation of osteoblasts (16), inhibit osteoclastogenesis (17), regulate estrogen levels (18), and regulate BMD and bone properties via certain pathways, such as the Wnt/β-catenin (19), NADPH oxidase 4/ROS/NF-κB (20) and TGF-β1/Smads signaling pathways (21). Furthermore, FLL also inhibits oxidative stress (22,23) and FLL has been reported to be associated with iron overload (24). The nuclear factor erythroid 2-related factor 2 (Nrf2)/heme oxygenase-1 (HO-1) signaling pathway is an important pathway against oxidative stress and regulates iron and lipid metabolism (25). Salidroside is the active ingredient found in FLL, which may protect against OP by promoting osteogenesis via the upregulation of Nrf2 (26). Nevertheless, whether the protective effect of FLL against PMOP is mediated by inhibiting ferroptosis through the Nrf2/HO-1 signaling pathway remains unclear. In the present study, a rat ovariectomy (OVX) model was established to assess the role of ferroptosis in PMOP and treatment with FLL in PMOP, thereby identifying potential targets for the prevention and treatment of OP.

Materials and methods

Experimental animals. A total of 15 female Sprague-Dawley rats (age, 9-10 weeks; weight, 250±20 g) were purchased from Sipeifu (Beijing) Biotechnology Co., Ltd. (animal certificate no. SCXK(Jing) 2021-0010). The rats were raised in conventional controlled conditions (22±1˚C; 50±5% relative humidity and 12 h light-dark cycle) and allowed free access to food and water. After acclimation for 1 week, the rats were randomly divided into three groups (n=5) as follows: SHAM, OVX and FLL group. Subsequently, surgery was performed on the rats under anesthesia using 3% pentobarbital sodium (45 mg/kg) by intraperitoneal injection. Bilateral ovaries were removed and ligatured in rats in the OVX and FLL groups. In the SHAM group, fat around the bilateral ovaries was ligatured. After recovering from the procedure, the animals were treated for 12 weeks. Rats in the SHAM and OVX groups were given water orally, while the FLL group were given FLL (1.56 g/kg/day) orally. After 12 weeks of treatment, the rats were anesthetized with 3% pentobarbital sodium (45 mg/kg) by intraperitoneal injection, followed by euthanasia by exsanguination (blood samples were collected from the abdominal aorta). After that, death was confirmed by no vital signs (pulse and breath). The uterus was removed and weighed. The uterus coefficient was calculated as follows: Uterus coefficient=uterus weight (mg)/body weight (g). The femurs were removed and preserved in 4% paraformaldehyde at room temperature for 48 h, and serum and tibia samples were maintained at -80˚C for use in further experiments.

Micro-CT. The right femur of all groups was scanned after removing the muscles and tissues. The scan area was set from the top of the femur to the lowest point of the lateral femoral knee growth plate using an X-ray energy of 70 kV, a current of 200 μA and a spatial resolution of 10.2 μm with a 2,016x1,344 image matrix, using a Skyscan 1276 micro-CT system (Bruker Corporation). Subsequently, detailed changes in femoral trabeculae were identified using histomorphometry. Using the lowest point of the lateral femoral knee growth plate as the baseline, an area with a thickness of 3 mm was selected as the region of interest to reconstruct 3D images using N-Recon (version 2.0.0.1; Bruker Corporation). The BMD, trabecular number (Tb.N), trabecular thickness (Tb.Th), trabecular bone separation (Tb.Sp), relative bone volume over total volume (BV/TV) and structure model index (SMI) were quantified using CTAn (version 1.5.6.2; Bruker Corporation).

Western blotting. Whole tibia samples were ground into powder in liquid nitrogen and were then lysed in RIPA protein lysis buffer (cat. no. C1053; Applygen Technologies, Inc.) with 2% protease inhibitor (cat. no. P1261; Beijing Solarbio Science & Technology Co., Ltd.) in a high-speed low-temperature tissue grinding machine (Wuhan Servicebio Technology Co., Ltd.). The supernatant was collected by centrifugation at 10,000 x g for 10 min at 4˚C, and the protein concentration of the supernatant was quantified using a BCA protein quantification kit (cat. no. 20201ES; Shanghai Yeasen Biotechnology Co., Ltd.). The supernatant was diluted according to the results of the BCA assay, mixed with loading buffer and then boiled for 10 min for denaturation. Protein samples (~40 μg/lane) were separated by 10% SDS-PAGE and transferred to a polyvinylidene fluoride membrane. Afterwards, the membranes were placed in TBS with 0.1% Tween-20, blocked with 5% skimmed milk at room temperature for 1 h and probed with primary antibodies against Nrf2 (1:5,000; cat. no. 16396-1-AP; Proteintech Group, Inc.), GPX4 (1:2,000; cat. no. 67763-1-Ig; Proteintech Group, Inc.) and β-actin (1:10,000; cat. no. 66009-1-Ig; Proteintech Group, Inc.) for 14 h at 4˚C. β-actin was used as the loading control. Subsequently, the protein bands were incubated at room temperature for 1 h with the HRP-conjugated goat anti-mouse (1:5,000; cat. no. ZB-2305; OriGene Technologies, Inc.) and anti-rabbit (1:5,000; cat. no. ZB-2301; OriGene Technologies, Inc.) secondary antibodies. Finally, the protein expression was visualized using a super sensitive ECL luminescent reagent (cat. no. MA0186; Dalian Meilun Biology Technology Co., Ltd.), assessed using a ChemiDoc XRS+ Gel Imaging System (Bio-Rad Laboratories, Inc.) and analyzed using Image Lab (version 6.1.0; Bio-Rad Laboratories, Inc.).

Reverse transcription-quantitative PCR (RT-qPCR). Total RNA was extracted from tibia samples using TRIzol Reagent (Takara Biotechnology Co., Ltd.) and the Nanodrop 8000 (Thermo Fisher Scientific, Inc.) was used to quantify the RNA. A total of 3 μg total RNA was utilized to synthesize complementary DNA sequences. Firstly, the oligo $(dT)_{18}$ primer (cat. no. 3806; Takara Biotechnology Co., Ltd.) and mRNA were incubated at 65˚C for 5 min and cooled on ice. Afterwards, the reaction buffer (cat. no. 2680Q; Takara Biotechnology Co., Ltd.), reverse transcriptase (cat. no. 2641A; Takara Biotechnology Co., Ltd.), dNTP (cat. no. 4030; Takara Biotechnology Co., Ltd.) and murine RNase inhibitor (cat. no. 10603ES10; Shanghai Yeasen Biotechnology Co., Ltd.) were added and samples were incubated at 42˚C for 1 h and at 70˚C for 5 min, then preserved at 4˚C temporarily. qPCR was performed using Hieff qPCR SYBR Green Master Mix (cat. no. 11203ES08; Shanghai Yeasen Biotechnology Co., Ltd.) with the following thermocycling conditions: Pre-denaturation at 95˚C for 10 min, followed by 40 cycles of denaturation at 95˚C for 5 sec, annealing at 60˚C for 30 sec and extension at 60˚C for 10 sec. The relative mRNA expression levels for each target gene were evaluated using the CFX Opus Real-Time PCR System (Bio-Rad Laboratories, Inc.). The mRNA expression levels of the target genes were standardized using GAPDH and quantified using the $2^{-\Delta\Delta Cq}$ method (27). The primers used for RT-qPCR are presented in Table I.

Fe^{2+} assay. Tibia samples (60 mg) were lysed and the supernatant was collected according to the aforementioned method for western blotting. The tissue total iron content colorimetric assay kit (cat. no. E1050; Applygen Technologies, Inc.) was used according to the manufacturer's instructions. Briefly, 100 μl mixed 4.5% potassium permanganate and buffer (1:1) solution was added to 100 μl supernatant and incubated at 60˚C for 1 h. The samples were then allowed to cool. A total of 30 μl detection solution was added, mixed and incubated at room temperature for 30 min. The solution was then centrifuged at 12,000 x g for 5 min at room temperature. A total of 200 μl supernatant was collected, and then the supernatant (200 μl per well) was added to a 96-well plate and quantified at 550 nm using a microplate reader.

Malondialdehyde (MDA) assay. Tibia samples were ground in liquid nitrogen and lysed in a pre-made cell lysis buffer for Western and IP (cat. no. P0013; Beyotime Institute of Biotechnology), then subjected to a lipid peroxidation MDA assay kit (cat. no. S0131S; Beyotime Institute of Biotechnology) for analysis. Briefly, the supernatant was collected according to the aforementioned method used for western blotting. Subsequently, 200 μl MDA working solution was added to 100 μl supernatant and the mixture was boiled for 15 min. After cooling to room temperature, the solution was centrifuged at 1,000 x g for 10 min at room temperature, and supernatant was collected and added to a 96-well plate (200 μl per well). Subsequently, quantification was performed at 532 nm using a microplate reader. Total protein concentration was measured using a BCA protein assay kit to calculate the content of MDA (μmol MDA/mg protein).

Table I. Sequences of primers used for reverse transcription-quantitative RT-qPCR.

Gene	Sequence (5'-3')
GAPDH	F: CATCTCCCTCACAATTCCATCC
	R: GAGGGTGCAGCGAACTTTAT
RUNX2	F: CTCCAGGAAGCCTTTGATACTC
	R: TAGGAGGGCTGGATCTTATGT
OSX	F: CCTACTTACCCGTCTGACTTTG
	R: CAACTGCCTTGGGCTTATAGA
Nrf2	F: ACGTGATGAGGATGGGAAAC
	R: TATCTGGCTTCTTGCTCTTGG
HO-1	F: GCATGAACTCTCTGGAGATGAC
	R: CAGCTCCTCAAACAGCTGAA
SLC7A11	F: CCTCTGTTCATCCCAGCATTAT
	R: CCCAGTCAAGGTGATAAGGAAG

F, forward; HO-1, heme oxygenase-1; Nrf2, nuclear factor erythroid 2-related factor 2; OSX, osterix; R, reverse; RUNX2, runt-related transcription factor 2; SLC7A11, solute carrier family 7 member 11.

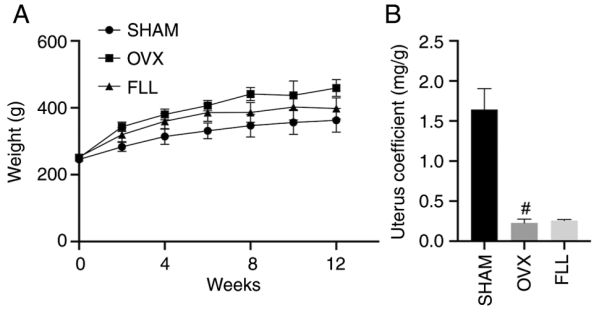

Figure 1. Changes in (A) weight and (B) uterus coefficient after OVX. #P<0.05 vs. SHAM. FLL, Fructus *Ligustri Lucidi*; OVX, ovariectomy.

Statistical analysis. Data are presented as the mean ± standard deviation (n=5). All data were checked for normality using the Kolmogorov-Smirnov test. Data were assessed using one-way ANOVA followed by Tukey's test using GraphPad Prism 9.00 (Dotmatics). P<0.05 was considered to indicate a statistically significant difference.

Results

FLL decreases the weight and increases the uterus coefficient in OVX rats. The body weight of all groups increased markedly between weeks 0 and 6 and remained steady in weeks 8-12. The OVX and FLL groups exhibited higher weight gain than the SHAM group, while the FLL group exhibited lower weight gain compared with the OVX group (Fig. 1A). The uterus coefficient of the OVX group was significantly lower compared with that of the SHAM group, while FLL slightly increased the uterus coefficient of the OVX rats; however, this was not statistically significant. Furthermore, the female rats exhibited atrophied uteri after OVX, which indicated that menopause was successfully induced (Fig. 1B).

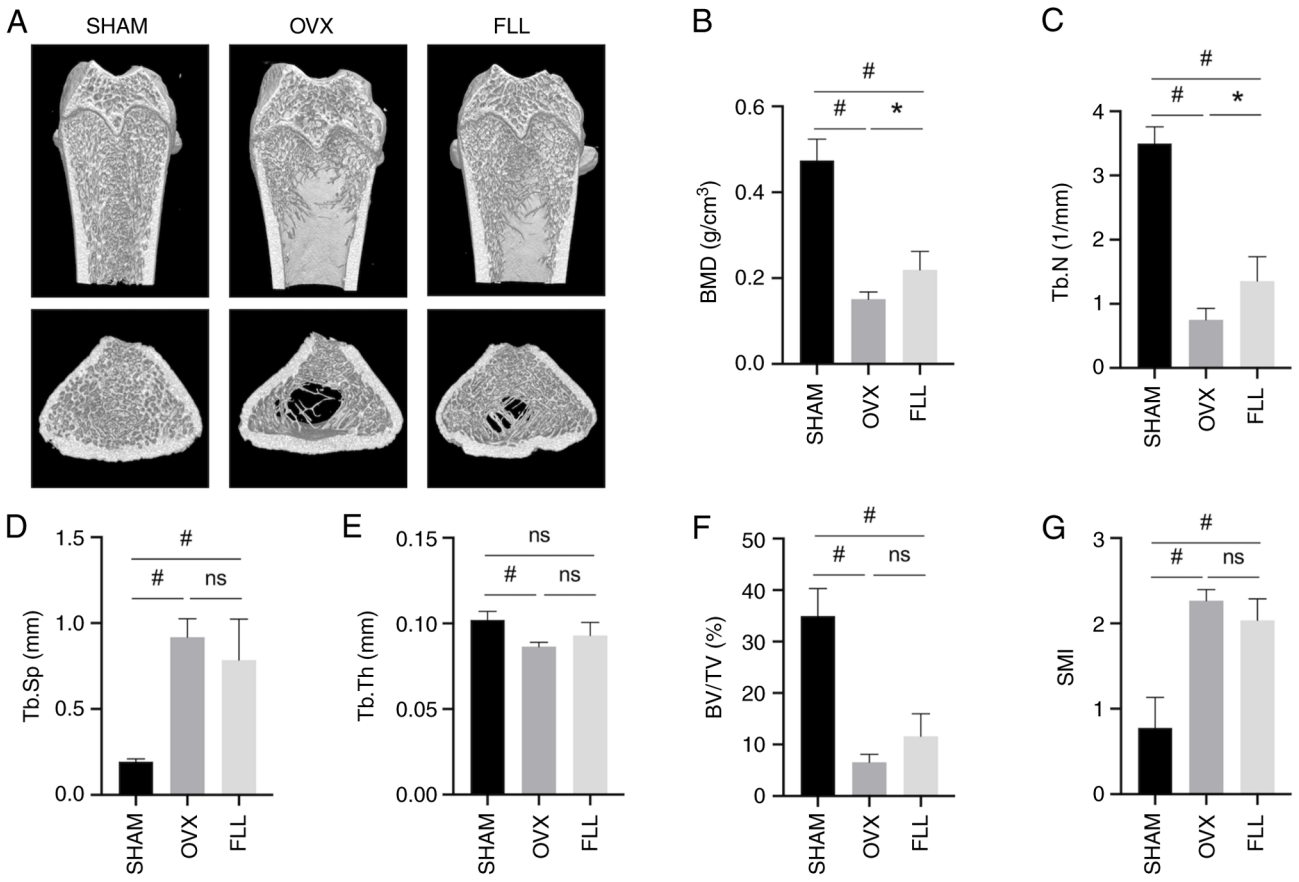

Figure 2. FLL improves bone architecture in OVX rats. (A) Micro-CT analysis of the distal femur region. (B) BMD, (C) Tb.N, (D) Tb.Sp, (E) Tb.Th, (F) BV/TV and (G) SMI. *P<0.05 vs. OVX; #P<0.05 vs. SHAM. BMD, bone mineral density; BV/TV, relative bone volume over total volume; FLL, Fructus *Ligustri Lucidi*; ns, not significant; OVX, ovariectomy; SMI, structure model index; Tb.N, trabecular number; Tb.Sp, trabecular bone separation; Tb.Th, trabecular thickness.

FLL improves the bone architecture of OVX rats. The severity of OP is directly reflected in the bone architecture, which was analyzed in the present study by micro-CT. The CT images showed fractured and decreased trabeculae of uneven thickness in the OVX group in comparison with the SHAM group, while the FLL group exhibited increased density and an increased number of trabeculae after 12 weeks of treatment (Fig. 2A). Furthermore, BMD, Tb.N, Tb.Th, Tb.Sp, BV/TV and SMI were analyzed to assess detailed changes in bone structure. The BMD and Tb. N data indicated significant bone loss in the OVX rats. Compared with the OVX group, BMD and Tb.N were significantly increased following FLL treatment, Tb.Th and BV/TV increased markedly but showed no statistical difference, and Tb.Sp and SMI decreased but showed no statistical difference. In addition, there was a significant difference in BMD, Tb.N, Tb.Sp, BV/TV and SMI when compared between the SHAM and FLL groups, which indicated that the FLL treatment partially restored bone structure (Fig. 2B-G).

FLL increases the expression levels of runt-related transcription factor 2 (RUNX2) and osterix (OSX) in OVX rats. Previous studies have reported that ferroptosis serves a crucial role in modulating bone metabolism by regulating osteoblasts (28,29). Thus, bone formation was analyzed in OVX and FLL rats. Osteoblasts greatly affect bone formation (30). The transcription factor runt-related protein family promotes the differentiation of osteoblasts from bone marrow mesenchymal stem cells (31). OSX is an osteoblast-specific transcription factor that is required for bone formation and was first reported to be a bone morphogenetic protein-2-inducible gene in mesenchymal stem cells (32). As shown in Fig. 3, the osteogenesis-related gene expression of RUNX2 and OSX was significantly decreased in the OVX group compared with the SHAM group, which was reversed after FLL administration, with a significant increase in the FLL group compared with the OVX group. These results indicated that FLL could recover the reduced osteogenic capacity induced by OVX to a certain extent.

FLL inhibits ferroptosis in OVX rats. Previous studies have reported a connection between ferroptosis and OP (29,33,34). In the present study, ferroptosis and decreased osteogenic function were observed in ovariectomized rats (Figs. 3 and 4). Excess iron promotes the generation of ROS during lipid peroxidation. Furthermore, activation of GPX4 and solute carrier family 7 member 11 (SLC7A11) inhibits ferroptosis by suppressing lipid peroxidation (35). The western blotting results showed significantly lower protein expression levels of GPX4 in the OVX group compared with the SHAM group (Fig. 4A). The RT-qPCR results demonstrated significantly lower mRNA expression levels of SLC7A11 in the OVX group compared with the SHAM group (Fig. 4B). Furthermore, the content of Fe^{2+} and MDA in bone tissues was significantly increased in the

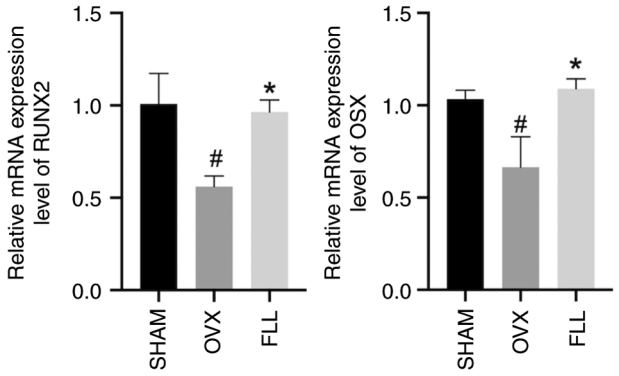

Figure 3. FLL increases the osteoblastic gene expression of RUNX2 and OSX. *P<0.05 vs. OVX; #P<0.05 vs. SHAM. FLL, Fructus *Ligustri Lucidi*; OSX, osterix; OVX, ovariectomy; RUNX2, runt-related transcription factor 2.

OVX group compared with the SHAM group, but significantly decreased compared with the OVX rats after FLL treatment (Fig. 4C). These results indicated the presence of ferroptosis in OVX rats and that FLL effectively inhibited ferroptosis.

FLL promotes the Nrf2/HO-1 signaling pathway in OVX rats. As a vital regulator of lipid peroxidation and ferroptosis, Nrf2 modifies downstream targets of GPX4 and SLC7A11. Nrf2 binds kelch like ECH associated protein 1 (Keap1) which is responsible for the cytosolic sequestration of Nrf2 under physiological conditions. Under stress conditions, Nrf2 is released from Keap1 and translocates to the nucleus, where Nrf2 exhibits a short half-life of ~200 min and is then degraded (25). HO-1, the enzyme responsible for catalyzing the conversion of heme into biliverdin, is upregulated by Nrf2 (36). Following OVX, Nrf2 and HO-1 were both significantly downregulated compared with the SHAM group, which was significantly reversed by FLL treatment (Fig. 5).

Discussion

The relationship between ferroptosis and OP has received growing attention, but only a small number of published papers have explored the relationship between ferroptosis and PMOP (10,29,33,37). The present study determined the presence of ferroptosis in OVX-induced OP in rats. In addition, the OVX rats were treated with FLL, and the results indicated that FLL protected against OP by inhibiting ferroptosis via the Nrf2/HO-1 signaling pathway.

In the bone remodeling process, the activities of osteoblasts and osteoclasts are in dynamic balance to maintain the homeostasis and integrity of bone tissues. Osteoblasts are mainly associated with bone reconstruction, involving the formation, mineralization and secretion of bone cells (30). The femur of OVX rats exhibited a low BMD, destroyed bone microarchitecture and downregulated expression of the transcription factors RUNX2 and OSX. These findings indicated dysfunctional bone formation in OVX-induced OP. Furthermore, micro-CT indicated that FLL promoted bone formation, increased the amount of trabecular bone and bone density, and improved bone histomorphology, which was consistent with previous reports (17,18). FLL treatment effectively recovered the expression of RUNX2 and OSX to similar levels compared with the SHAM group, which suggested that the therapeutic effect of FLL could be attributed to the promotion of bone formation.

The pathogenesis of PMOP is a complicated process and is still not fully understood. Previous studies have reported that ferroptosis serves a crucial role in OP (29,33,37). Ferroptosis, a form of programmed cell death, is characterized by the accumulation of intracellular iron and lipid ROS. Ferroptosis is mediated by the toxicity of free iron, the depletion of the antioxidant glutathione (GSH) and the accumulation of oxidative damage to membrane lipids (38). Although iron is essential for maintaining cell function, intracellular iron overload induces ROS formation through the Fenton reaction, generating deleterious lipid peroxides that damage the cellular structure and function. Among reactive lipid species produced by lipid peroxidation, 4-hydroxy-2-nonenal, MDA and other products can cause harm to cells (39). Furthermore, the System Xc-/GPX4 axis has been reported to serve a vital role in inhibiting ferroptosis. Firstly, cystine, the precursor of cysteine, is transported into the cell via System Xc-. Then, GSH is produced from cysteine, glutamate and glycine by enzymatic catalysis (40). SLC7A11 is a subunit of the solute transport family System Xc-transporter (41). GSH is a critical antioxidant in cells and is catalyzed by GPX4 to oxidize GSH during lipid peroxidation. Thereafter, H^+ is released to scavenge intracellular oxygen radicals and inhibit lipid peroxidation-induced ferroptosis (42). It has been previously reported that, in mice, ferroptosis exerts a marked impact on bone loss induced by a high-fat diet (29). Another study reported ferroptosis and increased mitochondrial ferritin in type 2 diabetic osteoporotic rats (37). The presence of iron has been reported to suppress the expression of RUNX2, the key transcription factor related to osteogenic differentiation (43). The anti-ferroptosis effect of 'Qing'e Pills' has been reported to be mediated by the upregulation of System Xc- and GPX4 in OVX rats (44). In essence, ferroptosis is mediated by lipid peroxidation and reduces expression of the core factors GPX4 and SLC7A11 in response to external stimuli, thereby impairing the antioxidant system. In the present study, increased levels of Fe^{2+} and MDA were observed in rat bone tissues 12 weeks after OVX, which indicated increased lipid peroxidation, leading to impaired cell metabolism (45). Western blotting indicated decreased protein expression levels of GPX4 and RT-qPCR indicated decreased mRNA expression levels of SLC7A11, which was consistent with a previous study (44). These results indicated that OVX could induce ferroptosis. A previous study reported that FLL could protect against OP by inhibiting oxidative stress (23). Significantly decreased Fe^{2+} and MDA levels and significantly increased levels of the marker factors GPX4 and SLC7A11 were observed in OVX rats treated with FLL compared with the OVX group. These findings suggested that FLL promoted osteogenesis and protected against PMOP by inhibiting ferroptosis.

The transcription factor Nrf2, one of the crucial regulators of the cellular antioxidant response, serves an essential role in protecting against oxidative stress (39). The antioxidant defense systems are closely associated with lipid accumulation (45). Due to its protective effect on maintaining cell

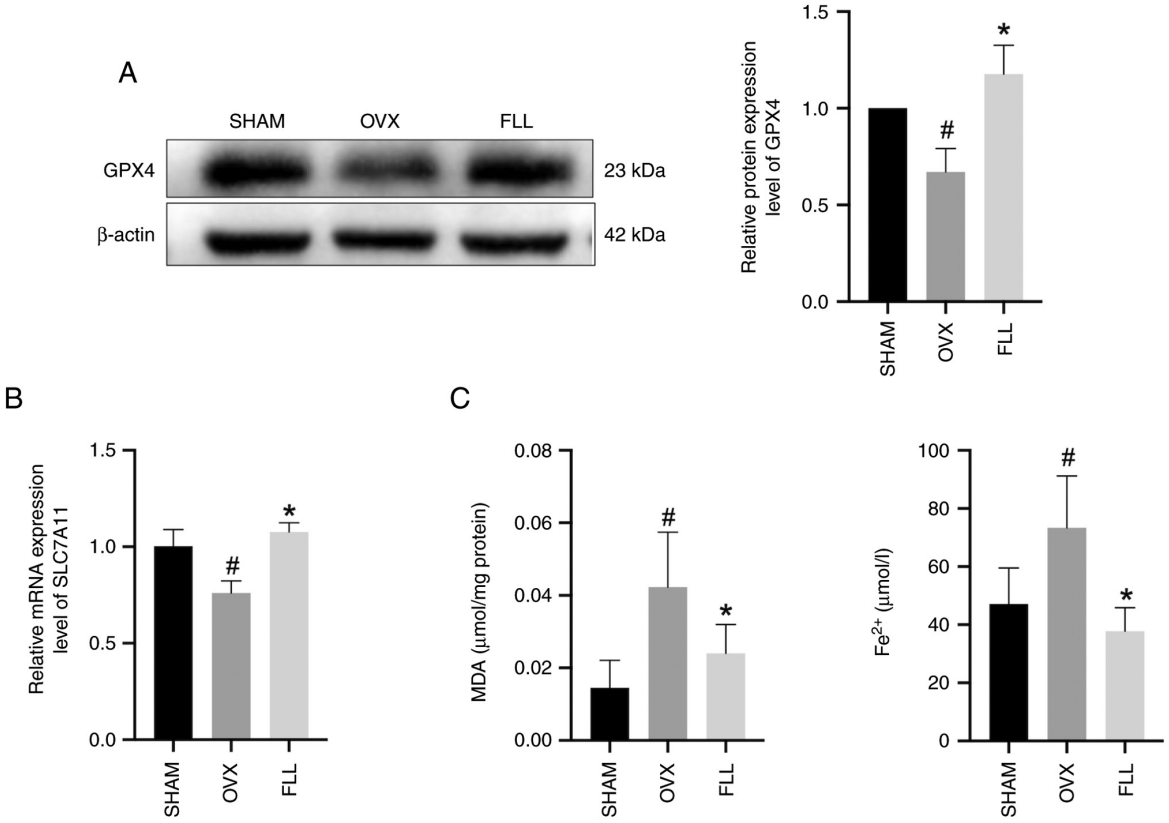

Figure 4. FLL increases the expression levels of GPX4 and SLC7A11, and decreases MDA and Fe^{2+} content. (A) FLL reversed the decrease in protein expression of GPX4 caused by OVX. (B) FLL increased SLC7A11 mRNA expression caused by OVX. (C) FLL reduced the Fe^{2+} and MDA content in bone tissues. *P<0.05 vs. OVX; #P<0.05 vs. SHAM. FLL, Fructus *Ligustri Lucidi*; GPX4, glutathione peroxidase 4; MDA, malondialdehyde; OVX, ovariectomy; SLC7A11, solute carrier family 7 member 11.

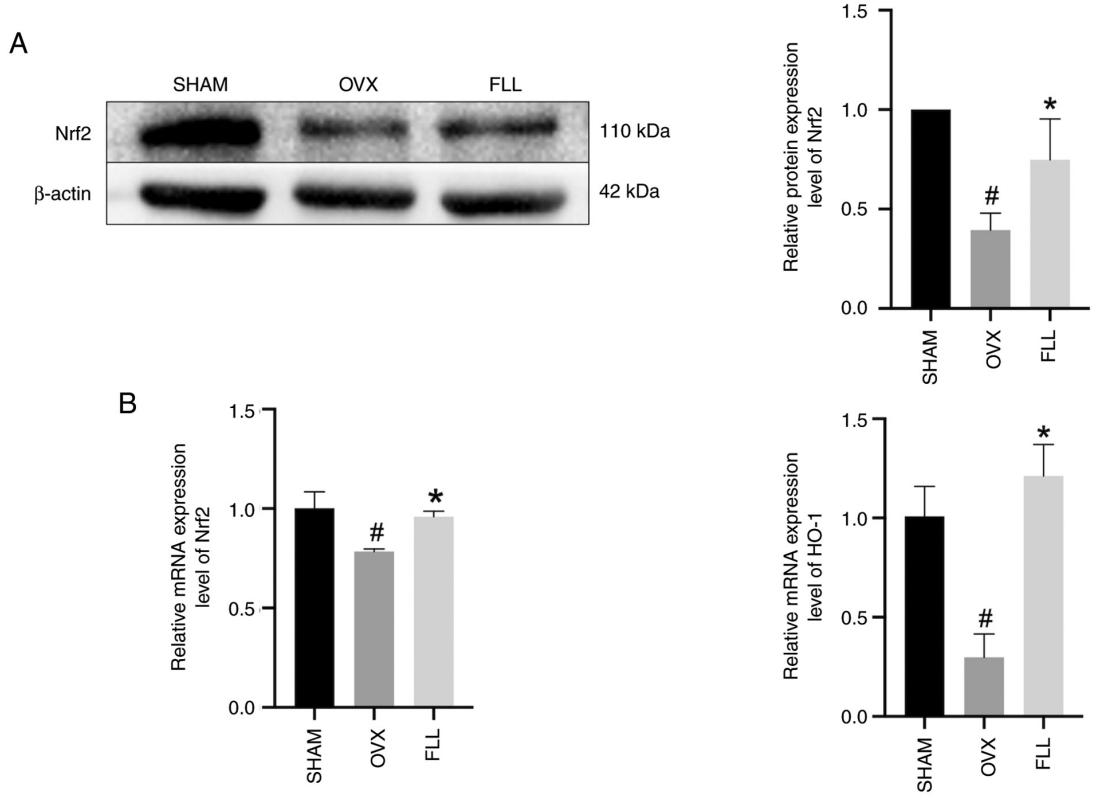

Figure 5. FLL activates the Nrf2/HO-1 signaling pathway. (A) FLL increased the protein expression levels of Nrf2 following OVX. (B) FLL increased Nrf2 and HO-1 mRNA expression levels in OVX rats. *P<0.05 vs. OVX; #P<0.05 vs. SHAM. FLL, Fructus *Ligustri Lucidi*; HO-1, heme oxygenase-1; Nrf2, nuclear factor erythroid 2-related factor 2; OVX, ovariectomy.

function, inhibition of Nrf2 or a number of its downstream target genes results in decreased responsiveness to cellular dysfunction and increased cell death (39). Following Nrf2 activation, HO-1 and other ROS-detoxifying enzymes are also upregulated (25). In the presence of oxidative stress, Nrf2 in the nucleus induces transcription of HO-1 and upregulates HO-1 gene and protein expression (46,47). However, downregulation of Nrf2 is associated with diseases associated with lipid peroxidation and ferroptosis (48). Previous studies have reported that the Nrf2/HO-1 signaling pathway is involved in the regulation of ferroptosis (34,49-51). Activation of the Nrf2/HO-1 signaling pathway may suppress the generation of intracellular lipid ROS and increase GPX4 activity, thereby protecting MC3T3-E1 cells against ferroptosis (34). Panaxydol has been reported to inhibit lipopolysaccharide-induced ferroptosis and inflammation through Keap1-Nrf2/HO-1 signaling (49). In conclusion, as the Nrf2/HO-1 pathway is activated, ferroptosis and cell injury are inhibited, restoring normal lipid metabolism (48). Consistent with the aforementioned reports, the present study demonstrated that Nrf2 and HO-1 were downregulated in OVX rats and signs of ferroptosis were observed in OVX rats, which indicated that the Nrf2/HO-1 signaling pathway may participate in OVX-induced ferroptosis. Salidroside, the active ingredient in FLL, has been previously reported to provide protection against OP by upregulating Nrf2 (26). Furthermore, FLL treatment significantly increased the expression levels of Nrf2, HO-1, GPX4 and SLC7A11, and Fe^{2+} and MDA content. Ferroptosis and lipid peroxidation were inhibited as the Nrf2/HO-1 signaling pathway was activated by FLL. These results indicated that the Nrf2/HO-1 signaling pathway could be an important factor in the regulation of OVX-induced OP and that the deactivation of the Nrf2/HO-1 signaling pathway corresponds with OVX-induced ferroptosis and OP.

In summary, the present study demonstrated that ferroptosis serves an essential role in the development of PMOP and may be a potential therapeutic target. The therapeutic effects of FLL in OP could be mediated by the activation of the Nrf2/HO-1 signaling pathway to inhibit ferroptosis. These findings may provide pharmacological and material evidence for clinical therapies for PMOP and form a foundation for further studies on the mechanism of iron-dependent ferroptosis and OP. However, the study had some limitations. The effect of FLL on OP may be achieved through complicated mechanisms, such as regulation of bone resorption (17). The study did not explore the detailed mechanism of FLL. Except for the Nrf2/HO-1 pathway, other pathways that may affect ferroptosis should also be explored. There are three main pathways that inhibit ferroptosis by acting on peroxide, including the System Xc-/GPX4, NADPH/ferroptosis suppressor protein 1/coenzyme Q10 and GTP cyclohydrolase 1/tetrahydrobioterin/phospholipid axes (40). The study only investigated the System Xc-/GPX4 axis. Experiments exploring the mechanism of ferroptosis in OVX-induced OP in detail should be conducted.

Acknowledgements

Not applicable.

Funding

The present study was supported by the China Academy of Chinese Medical Sciences Innovation Fund (grant no. CI 2021A00107), the National Natural Science Foundation of China (grant no. 82074297) and the Fundamental Research Funds for the Central Public Welfare Research Institutes (grant no. YZX-202244).

Availability of data and materials

The datasets used and/or analyzed during the current study are available from the corresponding author on reasonable request.

Authors' contributions

PL was responsible for project administration, data curation, development and design of the methodology, and writing the original draft of the manuscript. YW was responsible for data curation, data interpretation and project administration. QY was responsible for data curation, and the development and design of the methodology. YY was responsible for the development and design of the methodology, data validation, and data interpretation. RZ was responsible for project administration, data acquisition and data analysis. JM was responsible for data acquisition and data analysis. YC was responsible for supervision, data acquisition, data analysis and data validation. HL was responsible for funding acquisition, study design, supervision and writing the original draft of the manuscript. ZZ was responsible for conceptualization, funding acquisition, supervision, and reviewing and editing the manuscript. PL and HL confirm the authenticity of all the raw data. All authors read and approved the final manuscript.

Ethics approval and consent to participate

All experimental protocols were approved by the Ethics Committee of the Institute of Basic Theory of Chinese Medicine, China Academy of Chinese Medical Sciences (ethical approval no. IBTCMCACMS21-2202-02; Beijing, China).

Patient consent for publication

Not applicable.

Competing interest

The authors declare that they have no competing interests.

References

1. Song S, Guo Y, Yang Y and Fu D: Advances in pathogenesis and therapeutic strategies for osteoporosis. Pharmacol Ther 237: 108168, 2022.
2. Wang L, Yu W, Yin X, Cui L, Tang S, Jiang N, Cui L, Zhao N, Lin Q, Chen L, *et al*: Prevalence of osteoporosis and fracture in China: The China osteoporosis prevalence study. JAMA Netw Open 4: e2121106, 2021.
3. Hernlund E, Svedbom A, Ivergård M, Compston J, Cooper C, Stenmark J, McCloskey EV, Jönsson B and Kanis JA: Osteoporosis in the European Union: Medical management, epidemiology and economic burden. A report prepared in collaboration with the international osteoporosis foundation (IOF) and the European federation of pharmaceutical industry associations (EFPIA). Arch Osteoporos 8: 136, 2013.

4. Chen B, Li GF, Shen Y, Huang XI and Xu YJ: Reducing iron accumulation: A potential approach for the prevention and treatment of postmenopausal osteoporosis. Exp Ther Med 10: 7-11, 2015.
5. Fink HA, MacDonald R, Forte ML, Rosebush CE, Ensrud KE, Schousboe JT, Nelson VA, Ullman K, Butler M, Olson CM, *et al*: Long-term drug therapy and drug discontinuations and holidays for osteoporosis fracture prevention: A systematic review. Ann Intern Med 171: 37-50, 2019.
6. Kanis JA, Cooper C, Rizzoli R and Reginster JY; Scientific Advisory Board of the European Society for Clinical and Economic Aspects of Osteoporosis (ESCEO) and the Committees of Scientific Advisors and National Societies of the International Osteoporosis Foundation (IOF): European guidance for the diagnosis and management of osteoporosis in postmenopausal women. Osteoporos Int 30: 3-44, 2019.
7. Peng Z, Xu R and You Q: Role of traditional Chinese medicine in bone regeneration and osteoporosis. Front Bioeng Biotechnol 10: 911326, 2022.
8. Dixon SJ, Lemberg KM, Lamprecht MR, Skouta R, Zaitsev EM, Gleason CE, Patel DN, Bauer AJ, Cantley AM, Yang WS, *et al*: Ferroptosis: An iron-dependent form of nonapoptotic cell death. Cell 149: 1060-1072, 2012.
9. Liang C, Zhang X, Yang M and Dong X: Recent progress in ferroptosis inducers for cancer therapy. Adv Mater 31: e1904197, 2019.
10. Liu P, Wang W, Li Z, Li Y, Yu X, Tu J and Zhang Z: Ferroptosis: A new regulatory mechanism in osteoporosis. Oxid Med Cell Longev 2022: 2634431, 2022.
11. Jiang Z, Wang H, Qi G, Jiang C, Chen K and Yan Z: Iron overload-induced ferroptosis of osteoblasts inhibits osteogenesis and promotes osteoporosis: An in vitro and in vivo study. IUBMB Life 74: 1052-1069, 2022.
12. Xie Q, Sun Y, Xu H, Chen T, Xiang H, Liu H, Wang R, Tan B, Yi Q, Tian J and Zhu J: Ferrostatin-1 improves BMSC survival by inhibiting ferroptosis. Arch Biochem Biophys 736: 109535, 2023.
13. Li Y, Bai B and Zhang Y: Expression of iron-regulators in the bone tissue of rats with and without iron overload. Biometals 31: 749-757, 2018.
14. Kim BJ, Lee SH, Koh JM and Kim GS: The association between higher serum ferritin level and lower bone mineral density is prominent in women ≥45 years of age (KNHANES 2008-2010). Osteoporos Int 24: 2627-2637, 2013.
15. Cao M, Wu J, Peng Y, Dong B, Jiang Y, Hu C, Yu L and Chen Z: *Ligustri Lucidi* Fructus, a traditional Chinese medicine: Comprehensive review of botany, traditional uses, chemical composition, pharmacology, and toxicity. J Ethnopharmacol 301: 115789, 2023.
16. Kong Y, Ma X, Zhang X, Wu L, Chen D, Su B, Liu D and Wang X: The potential mechanism of Fructus *Ligustri Lucidi* promoting osteogenetic differentiation of bone marrow mesenchymal stem cells based on network pharmacology, molecular docking and experimental identification. Bioengineered 13: 10640-10653, 2022.
17. Ma Z, Tang X, Chen Y, Wang H, Li Y, Long Y and Liu R: Epimedii Folium and Ligustri *Lucidi Fructus* promote osteoblastogenesis and inhibit osteoclastogenesis against osteoporosis via acting on osteoblast-osteoclast communication. Oxid Med Cell Longev 2023: 7212642, 2023.
18. Tang YQ, Li C, Sun XJ, Liu Y, Wang XT, Guo YB, Wang LL, Ma RF, Niu JZ, Fu M, *et al*: Fructus *Ligustri Lucidi* modulates estrogen receptor expression with no uterotrophic effect in ovariectomized rats. BMC Complement Altern Med 18: 118, 2018.
19. Liu H, Guo Y, Zhu R, Wang L, Chen B, Tian Y, Li R, Ma R, Jia Q, Zhang H, *et al*: Fructus *Ligustri Lucidi* preserves bone quality through induction of canonical Wnt/β-catenin signaling pathway in ovariectomized rats. Phytother Res 35: 424-441, 2021.
20. Wang L, Ma R, Guo Y, Sun J, Liu H, Zhu R, Liu C, Li J, Li L, Chen B, *et al*: Antioxidant Effect of Fructus *Ligustri Lucidi* aqueous extract in ovariectomized rats is mediated through Nox4-ROS-NF-κB pathway. Front Pharmacol 8: 266, 2017.
21. Yang Y, Nian H, Tang X, Wang X and Liu R: Effects of the combined Herba Epimedii and Fructus *Ligustri Lucidi* on bone turnover and TGF-β1/Smads pathway in GIOP rats. J Ethnopharmacol 201: 91-99, 2017.
22. Li L, Chen B, Zhu R, Li R, Tian Y, Liu C, Jia Q, Wang L, Tang J, Zhao D, *et al*: Fructus *Ligustri Lucidi* preserves bone quality through the regulation of gut microbiota diversity, oxidative stress, TMAO and Sirt6 levels in aging mice. Aging (Albany NY) 11: 9348-9368, 2019.
23. Wu Y, Hu Y, Zhao Z, Xu L, Chen Y, Liu T and Li Q: Protective effects of water extract of Fructus *Ligustri Lucidi* against oxidative stress-related osteoporosis in vivo and in vitro. Vet Sci 8: 198, 2021.
24. Seo HL, Baek SY, Lee EH, Lee JH, Lee SG, Kim KY, Jang MH, Park MH, Kim JH, Kim KJ, *et al*: Liqustri lucidi Fructus inhibits hepatic injury and functions as an antioxidant by activation of AMP-activated protein kinase in vivo and in vitro. Chem Biol Interact 262: 57-68, 2017.
25. Loboda A, Damulewicz M, Pyza E, Jozkowicz A and Dulak J: Role of Nrf2/HO-1 system in development, oxidative stress response and diseases: An evolutionarily conserved mechanism. Cell Mol Life Sci 73: 3221-3247, 2016.
26. Wang YF, Chang YY, Zhang XM, Gao MT, Zhang QL, Li X, Zhang L and Yao WF: Salidroside protects against osteoporosis in ovariectomized rats by inhibiting oxidative stress and promoting osteogenesis via Nrf2 activation. Phytomedicine 99: 154020, 2022.
27. Livak KJ and Schmittgen TD: Analysis of relative gene expression data using real-time quantitative PCR and the 2(-Delta Delta C(T)) method. Methods 25: 402-408, 2001.
28. Zhao Y, Du Y, Gao Y, Xu Z, Zhao D and Yang M: ATF3 regulates osteogenic function by mediating osteoblast ferroptosis in type 2 diabetic osteoporosis. Dis Markers 2022: 9872243, 2022.
29. Zhu R, Wang Z, Xu Y, Wan H, Zhang X, Song M, Yang H, Chai Y and Yu B: High-fat diet increases bone loss by inducing ferroptosis in osteoblasts. Stem Cells Int 2022: 9359429, 2022.
30. Ponzetti M and Rucci N: Osteoblast differentiation and signaling: Established concepts and emerging topics. Int J Mol Sci 22: 6651, 2021.
31. Vimalraj S and Sekaran S: RUNX family as a promising biomarker and a therapeutic target in bone cancers: A review on its molecular mechanism(s) behind tumorigenesis. Cancers (Basel) 15: 3247, 2023.
32. Zhang C: Molecular mechanisms of osteoblast-specific transcription factor osterix effect on bone formation. Beijing Da Xue Xue Bao Yi Xue Ban 44: 659-665, 2012.
33. Li M, Yang N, Hao L, Zhou W, Li L, Liu L, Yang F, Xu L, Yao G, Zhu C, *et al*: Melatonin inhibits the ferroptosis pathway in rat bone marrow mesenchymal stem cells by activating the PI3K/AKT/mTOR signaling axis to attenuate steroid-induced osteoporosis. Oxid Med Cell Longev 2022: 8223737, 2022.
34. Ma H, Wang X, Zhang W, Li H, Zhao W, Sun J and Yang M: Melatonin suppresses ferroptosis induced by high glucose via activation of the Nrf2/HO-1 signaling pathway in type 2 diabetic osteoporosis. Oxid Med Cell Longev 2020: 9067610, 2020.
35. Stockwell BR, Friedmann Angeli JP, Bayir H, Bush AI, Conrad M, Dixon SJ, Fulda S, Gascón S, Hatzios SK, Kagan VE, *et al*: Ferroptosis: A regulated cell death nexus linking metabolism, redox biology, and disease. Cell 171: 273-285, 2017.
36. Zhang Q, Liu J, Duan H, Li R, Peng W and Wu C: Activation of Nrf2/HO-1 signaling: An important molecular mechanism of herbal medicine in the treatment of atherosclerosis via the protection of vascular endothelial cells from oxidative stress. J Adv Res 34: 43-63, 2021.
37. Wang X, Ma H, Sun J, Zheng T, Zhao P, Li H and Yang M: Mitochondrial ferritin deficiency promotes osteoblastic ferroptosis via mitophagy in type 2 diabetic osteoporosis. Biol Trace Elem Res 200: 298-307, 2022.
38. Bertrand RL: Iron accumulation, glutathione depletion, and lipid peroxidation must occur simultaneously during ferroptosis and are mutually amplifying events. Med Hypotheses 101: 69-74, 2017.
39. Dodson M, Castro-Portuguez R and Zhang DD: NRF2 plays a critical role in mitigating lipid peroxidation and ferroptosis. Redox Biol 23: 101107, 2019.
40. Duan JY, Lin X, Xu F, Shan SK, Guo B, Li FX, Wang Y, Zheng MH, Xu QS, Lei LM, *et al*: Ferroptosis and its potential role in metabolic diseases: A curse or revitalization? Front Cell Dev Biol 9: 701788, 2021.

41. Chai D, Zhang L, Xi S, Cheng Y, Jiang H and Hu R: Nrf2 activation induced by Sirt1 ameliorates acute lung injury after intestinal ischemia/reperfusion through NOX4-mediated gene regulation. Cell Physiol Biochem 46: 781-792, 2018.
42. Bachhawat AK and Yadav S: The glutathione cycle: Glutathione metabolism beyond the γ-glutamyl cycle. IUBMB Life 70: 585-592, 2018.
43. Balogh E, Tolnai E, Nagy B Jr, Nagy B, Balla G, Balla J and Jeney V: Iron overload inhibits osteogenic commitment and differentiation of mesenchymal stem cells via the induction of ferritin. Biochim Biophys Acta 1862: 1640-1649, 2016.
44. Hao J, Bei J, Li Z, Han M, Ma B, Ma P and Zhou X: Qing'e pill inhibits osteoblast ferroptosis via ATM serine/threonine kinase (ATM) and the PI3K/AKT pathway in primary osteoporosis. Front Pharmacol 13: 902102, 2022.
45. Gaschler MM and Stockwell BR: Lipid peroxidation in cell death. Biochem Biophys Res Commun 482: 419-425, 2017.
46. Baird L, Swift S, Llères D and Dinkova-Kostova AT: Monitoring Keap1-Nrf2 interactions in single live cells. Biotechnol Adv 32: 1133-1144, 2014.
47. Baird L, Llères D, Swift S and Dinkova-Kostova AT: Regulatory flexibility in the Nrf2-mediated stress response is conferred by conformational cycling of the Keap1-Nrf2 protein complex. Proc Natl Acad Sci USA 110: 15259-15264, 2013.
48. Dong H, Qiang Z, Chai D, Peng J, Xia Y, Hu R and Jiang H: Nrf2 inhibits ferroptosis and protects against acute lung injury due to intestinal ischemia reperfusion via regulating SLC7A11 and HO-1. Aging (Albany NY) 12: 12943-12959, 2020.
49. Li J, Lu K, Sun F, Tan S, Zhang X, Sheng W, Hao W, Liu M, Lv W and Han W: Panaxydol attenuates ferroptosis against LPS-induced acute lung injury in mice by Keap1-Nrf2/HO-1 pathway. J Transl Med 19: 96, 2021.
50. Chen Y, Zhang P, Chen W and Chen G: Ferroptosis mediated DSS-induced ulcerative colitis associated with Nrf2/HO-1 signaling pathway. Immunol Lett 225: 9-15, 2020.
51. Dang R, Wang M, Li X, Wang H, Liu L, Wu Q, Zhao J, Ji P, Zhong L, Licinio J and Xie P: Edaravone ameliorates depressive and anxiety-like behaviors via Sirt1/Nrf2/HO-1/Gpx4 pathway. J Neuroinflammation 19: 41, 2022.